BioOne COMPLETE

Validating Radiosensitivity with Pre-Exposure Differential Gene Expression in Peripheral Blood Predicting Survival and Non-Survival in a Second Irradiated Rhesus Macaque Cohort

Authors: Schwanke, D., Fatanmi, O. O., Wise, S. Y., Ostheim, P., Schüle, S., et al.

Validating Radiosensitivity with Pre-Exposure Differential Gene Expression in Peripheral Blood Predicting Survival and Non-Survival in a Second Irradiated Rhesus Macaque Cohort

D. Schwanke,[a] O. O. Fatanmi,[b,c] S. Y. Wise,[b,c] P. Ostheim,[a] S. Schüle,[a] G. Kaletka,[a] S. Stewart,[a] T. Wiegel,[d] V. K. Singh,[b,c,1] M. Port,[a] M. Abend[a,1]

[a] Bundeswehr Institute of Radiobiology, Munich, Germany; [b] Division of Radioprotectants, Department of Pharmacology and Molecular Therapeutics, F. Edward Hébert School of Medicine, and [c] Armed Forces Radiobiology Research Institute, Uniformed Services University of the Health Sciences, Bethesda, Maryland; [d] Department of Radiation Oncology, University Hospital, Ulm, Germany

Schwanke D, Fatanmi OO, Wise SY, Ostheim P, Schüle S, Kaletka G, Stewart S, Wiegel T, Singh VK, Port M, Abend M. Validating Radiosensitivity with Pre-Exposure Differential Gene Expression in Peripheral Blood Predicting Survival and Non-Survival in a Second Irradiated Rhesus Macaque Cohort. Radiat Res. 201, 384–395 (2024).

Radiosensitivity differs in humans and possibly in closely related nonhuman primates. The reasons for variation in radiosensitivity are not well known. In an earlier study, we examined gene expression (GE) pre-radiation in peripheral blood among male (n = 62) and female (n = 60) rhesus macaques (n = 122), which did or did not survive (up to 60 days) after whole-body exposure of 7.0 Gy ($LD_{66/60}$). Eight genes (*CHD5, CHI3L1, DYSF, EPX, IGF2BP1, LCN2, MBOAT4, SLC22A4*) revealed significant associations with survival. Access to a second rhesus macaque cohort (males = 40, females = 23, total n = 63) irradiated with 5.8–7.2 Gy ($LD_{29-50/60}$) and some treated with gamma-tocotrienol (GT3, a radiation countermeasure) allowed us to validate these gene expression changes independently. Total RNA was isolated from whole blood samples and examined by quantitative RT-PCR on a 96-well format. cycle threshold (Ct)-values normalized to 18S rRNA were analyzed for their association with survival. Regardless of the species-specific TaqMan assay, similar results were obtained. Two genes (*CHD5* and *CHI3L1*) out of eight revealed a significant association with survival in the second cohort, while only *CHD5* (involved in DNA damage response and proliferation control) showed mean gene expression changes in the same direction for both cohorts. No expected association of *CHD5* GE with dose, treatment, or sex could be established. Instead, we observed significant associations for those comparisons comprising pre-exposure samples with *CHD5* Ct values ≤ 11 (total n = 17). *CHD5* Ct values ≤ 11 in these comparisons were mainly associated with increased frequencies (61-100%) of non-survivors, a trend which depending on the sample numbers, reached significance (P = 0.03) in males and, accordingly, in females. This was also reflected by a logistic regression model including all available samples from both cohorts comprising *CHD5* measurements (n = 104, odds ratio 1.38, 95% CI 1.07–1.79, P = 0.01). However, this association was driven by males (odds ratio 1.62, 95% CI 1.10–2.38, P = 0.01) and *CHD5* Ct values ≤ 11 since removing low *CHD5* Ct values from this model, converted to insignificance (P = 0.19). A second male subcohort comprising high *CHD5* Ct values ≥ 14.4 in both cohorts (n = 5) appeared associated with survival. Removing these high *CHD5* Ct values converted the model borderline significant (P = 0.051). Based on the probability function of the receiver operating characteristics (ROC) curves, 8 (12.3%) and 5 (7.7%) from 65 pre-exposure RNA measurements in males, death and survival could be predicted with a negative and positive predictive value ranging between 85–100%. An associated odds ratio reflected a 62% elevated risk for dying or surviving per unit change (Ct-value) in gene expression, considering the before-mentioned *CHD5* thresholds in RNA copy numbers. In conclusion, we identified two subsets of male animals characterized by increased (Ct values ≤ 11) and decreased (Ct values ≥ 14.4) *CHD5* GE copy numbers before radiation exposure, which independently of the cohort, radiation exposure or treatment appeared to predict the death or survival in males. © 2024 by Radiation Research Society

[1] Corresponding authors: Michael Abend, email: michaelabend@bundeswehr.org, and Vijay K. Singh, email: vijay.singh@usuhs.edu.

INTRODUCTION

Inter-individual differences in radiation resistance and radiation sensitivity ("radiosensitivity") after exposure to ionizing radiation is important to study. Nevertheless, the nature of the underlying variation in radiosensitivity among individuals is poorly understood.

It is well known that ionizing radiation is described as a two-edged sword (1). On the one hand, ionizing radiation is well known for its potential to control tumor cell growth in radiotherapy. On the other hand, its potential to cause stochastic (e.g., tumors) and deterministic health effects like the (hematopoietic) acute radiation syndrome (H-ARS) has long been known. In the latter case, for instance, with a whole-body exposure of 3–4 Gy ($LD_{50/60}$), about 50% of humans will die from ARS within 60 days without treatment (2). Knowing that this dose provides a 50% chance of predicting the clinical outcome, which underlines the complexity of

384

this issue. The relation of exposure to radiation with ARS depends on several factors, including radiation exposure characteristics (e.g., radiation quality, fractionation, dose rate, partial-/total-body exposure), inherent biological processes (e.g., cell cycle dependency, oxygenation) (3), as well as other aspects such as radiosensitivity or pre-exposure health conditions. We hypothesize that the individual transcriptional makeup of a person at the time of the radiation exposure may determine radiation sensitivity (or resistance) of individuals.

Understanding the individual human responses to radiation exposure with respect to tissue damage or developing radiation-related sequelae would be of benefit in several instances. For example, manned space projects like the ARTEMIS mission would prosper from knowing the individual radiosensitivity in selecting potential astronauts (4). Furthermore, the diagnostic windows in radiotherapy could be widened, and individual specific radiotherapy might be applied when the radiosensitivity of patient's tumors and normal tissue would be predicted a priori (5–7). Concerning preparedness against radiological/nuclear (RN) mass casualties, such as dirty-bomb or atomic-bomb scenarios, individuals exposed to the same magnitude of radiation might develop different degrees of life-threatening ARS. Knowing about individual radiosensitivity could guide the treating physicians in choosing the appropriate therapy (8). Hence the question arises whether the transcriptional status of cells prior to radiation exposure influences the degree of radiation damage or H-ARS severity?

There are indications that the radiation-induced cancer risk differs among females and males (9, 10), and between some ethnicities, as shown, e.g., with breast or prostate cancer (11, 12). Animal studies suggest a difference in sex in the response to certain dose regarding hematologic acute radiation syndrome (13–15).

In previous work in a male baboon model, several promising micro-RNAs (miRNA) addressing the H-ARS endpoint could be detected (16). miRNA has also been investigated using male and female rhesus macaques and total-body gamma irradiation. Results of this study suggested that female rhesus macaques may to be more sensitive to radiation, but the difference was not significant (17). In a further study, radiosensitivity with the endpoint survival and non-survival after total-body irradiation (TBI) in 122 male and female rhesus macaques (18) was evaluated. Hereby, eight candidate genes associated with survival could be independently validated.

In collaboration with Armed Forces Radiobiology Research Institute (AFRRI), we accessed a second rhesus macaque cohort comprising pre-exposure blood samples of 63 male and female rhesus macaques. The individual animals were exposed to 5.8–7.2 Gy of radiation (TBI) corresponding to $\sim LD_{30-70/60}$. These nonhuman primates (NHP) were either untreated (placebo) or treated with different doses of a potential medical countermeasure, gamma-tocotrienol (GT3) (19–23). These rhesus macaques enabled an independent validation of eight already identified radiosensitivity (survival) predicting genes in a second cohort. Due to the close homology

of the human and rhesus macaque species, in addition to the well-characterized human transcriptome, a gene detection assay based on the human genome was employed in rhesus macaques in the previous study. As well as these assays, complimentary gene detection assays using the rhesus macaque transcriptome were generated and examined within this validation study. We hypothesized that the pre-exposure transcription status of the cells at the time of exposure would impact survival, thus, reflecting differences in radiosensitivity (identifying non-survivor) or radioresistance (identifying survivor). This is probably the most robust parameter in nature: cell death or, regarding an organism, survival and non-survival.

MATERIALS AND METHODS

Animals and Irradiation

Rhesus Macaque Cohort 1

For inter-species comparison, we used qRT-PCR gene expression (GE) data [low-density array (LDA)] of the eight genes, which were examined on 122 specimens (males = 62; females = 60) of our previously investigated first cohort (herein referred to as cohort 1). After 7 Gy TBI, about two-thirds survived ($LD_{66/60}$, Table 1). Rhesus macaques were either non-treated or treated with interleukin 12, granulocyte-colony stimulating factor, or a combination of both (Table 1). Further information regarding the cohort and the used material and methods are described elsewhere (18).

Rhesus Macaque Cohort 2

Animals

For second cohort, a total of 64 healthy rhesus macaques (*Macaca mulatta,* Chinese substrain) were obtained from the National Institutes of Health Animal Center (NIHAC, Poolesville, MD, Table 1). The animals were quarantined for 6–7 weeks prior to the beginning of the experiment. One rhesus macaque was excluded from the study due to a viral infection, leaving 63 rhesus macaques eligible for this study. Overall, there were 40 male and 23 female clinically healthy animals weighing 3.6–8.4 kg and were housed at AFRRI (Bethesda, MA). All animals were kept in a facility accredited by the Association for Assessment and Accreditation of Laboratory Animal Care (AAALAC) International. Housing requirements, sensory and dietary enrichment details have been described in detail previously (24, 25). Single housing was utilized for the animals for this study and justification for single housing is described earlier (26). All of the procedures performed in this study were in accordance with the animal use protocols approved by the Institutional Animal Care and Use Committee (IACUC, AFRRI) and Department of Defense second-tier approval from the Animal Care and Use Review Office (ACURO). The study was reported in accordance with ARRIVE (Animal Research: Reporting of In Vivo Experiments) guidelines and with the recommendations made in the Guide for the Care and Use of Laboratory Animals (27).

Drug Preparation and Administration

Gamma-tocotrienol was procured from (American River Nutrition, Hadley, MA, ExcelVite Sdn. Bhd., Perak, Malaysia) and its preparation and administration have been described earlier (28). The dose used in this study range from 37.5 mg/kg and the volume administered to each animal was based on individual animal body weight. At least 24–48 h prior to drug administration, the injection site (dorsal scapular area) was shaved and cleaned to monitor for any skin irritations or abscess formation. GT3 and or vehicle administrations were performed with a sterile 21–25 gauge needle length of 3/4–1″.

TABLE 1
Overview Regarding Rhesus Macaques Used in Two Different Cohorts

Sex	Radiation exposure (Gy)	Treatment group	Survival status	Number of animals	Sex	Radiation exposure (Gy)	Treatment group	Survival status	Number of animals
Cohort 1				**122**	*Cohort 2*				**63**
males				**62**	males				**20**
	7	treated		44		5.8	treated		10
			survivor	25				survivor	7
			non-survivor	19				non-survivor	3
		untreated		18			untreated		10
			survivor	6				survivor	7
			non-survivor	12				non-survivor	3
					males				**4**
						6.5	treated		3
								survivor	3
							untreated		1
								survivor	1
					males				**16**
						7.2	untreated		16
								survivor	8
								non-survivor	8
females				**60**	females				**11**
	7	treated		42		5.8	treated		6
			survivor	16				survivor	5
			non-survivor	26				non-survivor	1
		untreated		18			untreated		5
			survivor	3				survivor	3
			non-survivor	15				non-survivor	2
					females				**12**
						6.5	treated		5
								survivor	2
								non-survivor	3
							untreated		7
								survivor	5
								non-survivor	2

Notes. The total number of animals is provided considering sex, radiation exposure, treatment and survival. Gamma tocotrienol (GT3) used for treatment in this study is a promising medical countermeasure under development and has demonstrated consistent efficacy in murine and rhesus macaque models. However, for this study, new vendors of GT3 were selected and the specific formulation used in this study was found not to be efficacious. This was likely due to phase separation (unstable emulsion) of GT3 when prepared as an injectable suspension. This issue has since been resolved and studies for the advanced development of GT3 are continuing.

Blood Sample Collection

Either seven or one day before irradiation blood was collected by venipuncture from either the saphenous or cephalic vein of the lower leg or from the brachial vein from the upper extremity of the arm. From rhesus macaques of cohort 2, 1 ml of peripheral blood was drawn into PAXgene Blood RNA tubes (PreAnalytiX, a Qiagen/Becton, Dickinson and Company, Franklin Lakes, NJ). After collection, the blood was mixed immediately by inverting the tube 10 times. The tubes were maintained at room temperature in the laboratory overnight and were later stored at –80°C until analysis (*29*).

Irradiation

Prior to the irradiation procedure, does rate measurements were performed and its description have been provided earlier (*30, 31*). The animals were fasted for at least 12–18 h prior to irradiation, and at approximately 30-45 min before exposure, all animals received appropriate anesthetics. All details for irradiation procedure have been discussed previously (*32*). Three different dose groups of 5.8 Gy (n = 31, males n = 20 and females n = 11), 6.5 Gy (n = 16, males n = 4 and females n = 12), and 7.2 Gy (n = 16 males) were used for this study. After the procedure, once the animals were certified to be in stable condition, they were transported back to the housing cages where they completed their recovery.

Euthanasia

After irradiation, animals are prone to exhibit clinical ARS-related signs and symptoms, and daily observations were increased to three times a day (no more than 10 h apart) during the critical period (days 10–20 postirradiation) to assess for moribundity. If an animal reached a state of moribundity, the animal was euthanized. As a surrogate for mortality, moribundity was used for assessment of animals, and were euthanized to minimize pain and distress. All euthanasia criteria and additional details have been provided previously (*33*). In general, euthanized NHPs

TABLE 2

Presented are the P values from Statistical Comparisons of Gene Expression-Difference Between Survivor and Non-Survivor for the Eight Investigated Genes for Cohort 1 and 2 (Parametrical t-test- or Non-Parametrical Man-Whitney Rank-Sum Test where Applicable)

					Statistical differences among survivor vs non-survivor (p-values)																Number of CHD5 HS with Ct ≤ 11*	
					EPX		LCNS		MBOAT4		DYSF		SLC22A4		IGF2BP1		CHI3L1		CHD5			
Dose(Gy)	Sex	Treatment	# Survivors	# Non-survivors	Hs	Rm	Hs	Rm	Hs	Rm	Hs	Rm	Hs	Rm	Hs	Rm	Hs	Rm	Hs	Rm	Surv	Nonsurv
Cohort 1																						
7	females	combined	14-5	27-11	0.7	–	0.37	–	***0.0004***	–	0.2	–	0.9	–	0.6	–	0.7	–	0.9	–	0	1
	males		23-16	14-9	***0.01***	–	***0.007***	–	0.3	–	***0.04***	–	***0.03***	–	0.2	–	***0.046***	–	***0.006***	–	1	2
Cohort 2																						
5.8-7.2	females	combined	15	8	0.7	0.5	0.1	0.2	0.7	0.7	0.4	0.3	0.2	0.3	0.5	0.6	***0.09***	***0.09***	***0.09***	***0.08***	4	4
	males		26-25	14	0.7	0.7	0.2	0.2	0.2	0.2	0.3	0.2	0.8	0.8	0.7	0.5	0.6	0.6	0.2	0.2	1	4
5.8	females	untreated	3	2	0.5	0.5	0.1	0.1	1.0	0.7	0.6	1.0	0.6	0.9	0.3	0.2	0.4	0.4	0.9	0.9	1	1
		treated	5	1	0.2	0.3	0.6	0.6	0.6	0.6	0.9	0.9	0.4	0.5	0.7	0.6	0.9	0.9	0.8	0.7	2	0
	males	untreated	7	3	0.6	0.5	0.7	0.7	0.1	0.2	0.7	0.7	0.4	0.7	0.9	0.9	0.2	0.2	0.9	0.9	1	0
		treated	7	3	0.3	0.3	0.9	0.9	1.0	0.9	0.8	0.8	0.5	0.6	***0.03***	***0.01***	0.7	0.4	0.7	***0.045***	0	2
6.5	females	untreated	5	2	0.9	0.9	0.6	0.7	0.6	0.6	0.7	0.7	0.8	0.6	0.1		***0.09***	***0.07***	***0.06***		0	2
		treated	2	3	0.6	0.6	0.2	0.1	0.7	0.6	0.4	0.4	0.9	0.7	0.7	0.8	0.2	***0.06***	0.4	0.4	1	1
7.2	males	untreated	8	8	0.9	0.9	0.2	0.3	***0.06***	***0.06***	0.7	0.6	0.6	0.5	0.9	0.8	0.6	0.6	0.3	0.6	0	2

In addition, the results of the rhesus monkey assay are listed for cohort 2. Further analysis considering treatment and absorbed dose were performed for cohort 2. All comparisons were performed separately by sex. The last column depicts the number of animals where *CHD5* ≤ 11 values were measured in survivors and non-survivors employing the human TaqMan assay (Hs). The corresponding fold changes in gene expression are presented in supplementary Table S2; https://doi.org/10.1667/RADE-23-00099.1.S2.

were defined as non-survivors (n = 22), while all living animals on day 60 were euthanized and considered as survivors (n = 41).

RNA-Extraction and Quality-Control

Filled PAXgene® Blood RNA tubes were manually thawed, centrifuged, the supernatant discarded, and pellets resuspended with proteinase K augmented buffers. RNA from PAXgene Blood RNA tubes was isolated semi-automatically following the QIAsymphony® Blood RNA Kit (QIAGEN, Hilden, Germany) using the QIAsymphony SP (QIAGEN, Hilden, Germany). This procedure uses the RNA-binding silica surface of magnetic beads. After several washing and digestion steps with DNase I and proteinase K, RNA was isolated automatically, eluted in 80 µl BR5 buffer, heated to 65C for five min, and stored at −20°C.

For quantification, RNA-eluates were measured spectrophotometrically (NanoDrop™, PeqLab Biotechnology, Erlangen, Germany). DNA contamination was precluded via PCR using primers for the β-actin gene. qRT-PCR was performed on all specimens with a ratio of A260/A280 nm ≥ 2.0. The quality was addressed by automated electrophoretic integrity measurements (4200 TapeStation System, Agilent Technologies, Santa Clara, CA), and RIN (RNA integrity number) values were calculated. Questionable measurements were confirmed via 18S rRNA-qRT-PCR. Only samples meeting predefined quality criteria [e.g., 18S rRNA-raw cycle-threshold (Ct) values (0.01 ng/reaction) ranging between 20 and 23 are expected for successful qRT-PCR] were further processed, leading to the qRT-PCR.

Quantitative Real-Time Reverse Transcription Polymerase Chain Reaction (qRT-PCR)

Aliquots of total RNA (0.6–1 µg) were reverse transcribed with the High-Capacity cDNA Reverse Transcription Kit (Applied Biosystems™, Life Technologies, Darmstadt, Germany). Equal amounts of template cDNA (10 ng) were used per reaction, mixed with the TaqMan® Universal PCR Master Mix, and gene-specific TaqMan™ Assays were added (Supplementary Table S1, https://doi.org/10.

1667/RADE-23-00093.1.S1).[2] We used standard human TaqMan™ Assays from our former study (18). Corresponding rhesus monkey TaqMan™ Assays (Rm) were generated using the same exon regions. The qRT-PCR was performed on a 96-well format using the QuantStudio™ 12K OA Real-Time PCR System (Thermo Fisher SCINTIFIC Inc., Waltham, MA). The raw cycle threshold was normalized to the diluted 18S rRNA. After normalization, fold change (FC) differences in gene expression between survivors and non-survivors were calculated by the ΔΔ Ct-approach (FC = $2^{-\Delta\Delta CT}$) relative to non-survivors used as the calibrator. The fold change refers to several-fold of over or under expression relative to the calibrator. Genes were assumed to be differentially expressed if $0.5 \geq FC \geq 2$ (16, 34).

Statistical Analysis

Results were presented as normalized Ct values. Intra- and inter-cohort comparisons were performed by the parametrical t-test or the non-parametrical Mann-Whitney Rank Sum test, where applicable. Differences in variance distribution among compared groups were calculated using the Brown-Forsythe test. The chi-square statistics or Fischer's exact test investigated differences in the frequency distribution. Logistic regression and receiver operating characteristics with an odds ratio (OR) and 95% confidence interval (CI), as well as positive and negative predictive values, were calculated for the prediction of survival and non-survival, respectively. P values < 0.05 were defined as significant, and P values ≥ 0.05 but < 0.1 as borderline significant. For inter-cohort comparisons of chromodomain helicase DNA-binding protein 5 (*CHD5*) normalized Ct values generated by low-density array technology in cohort 1 and 96-well format qRT-PCR in cohort 2, Ct values had to be aligned by subtracting 2.96 Ct values from cohort 1 (median Ct-difference of cohort 2 male non-survivors [12.45] from cohort 1 male non-survivors [15.41]). For statistical analyses and

[2] Editor's note. The online version of this article (DOI: https://doi.org/10.1667/RADE-23-00099.1.S1) contains supplementary information that is available to all authorized users.
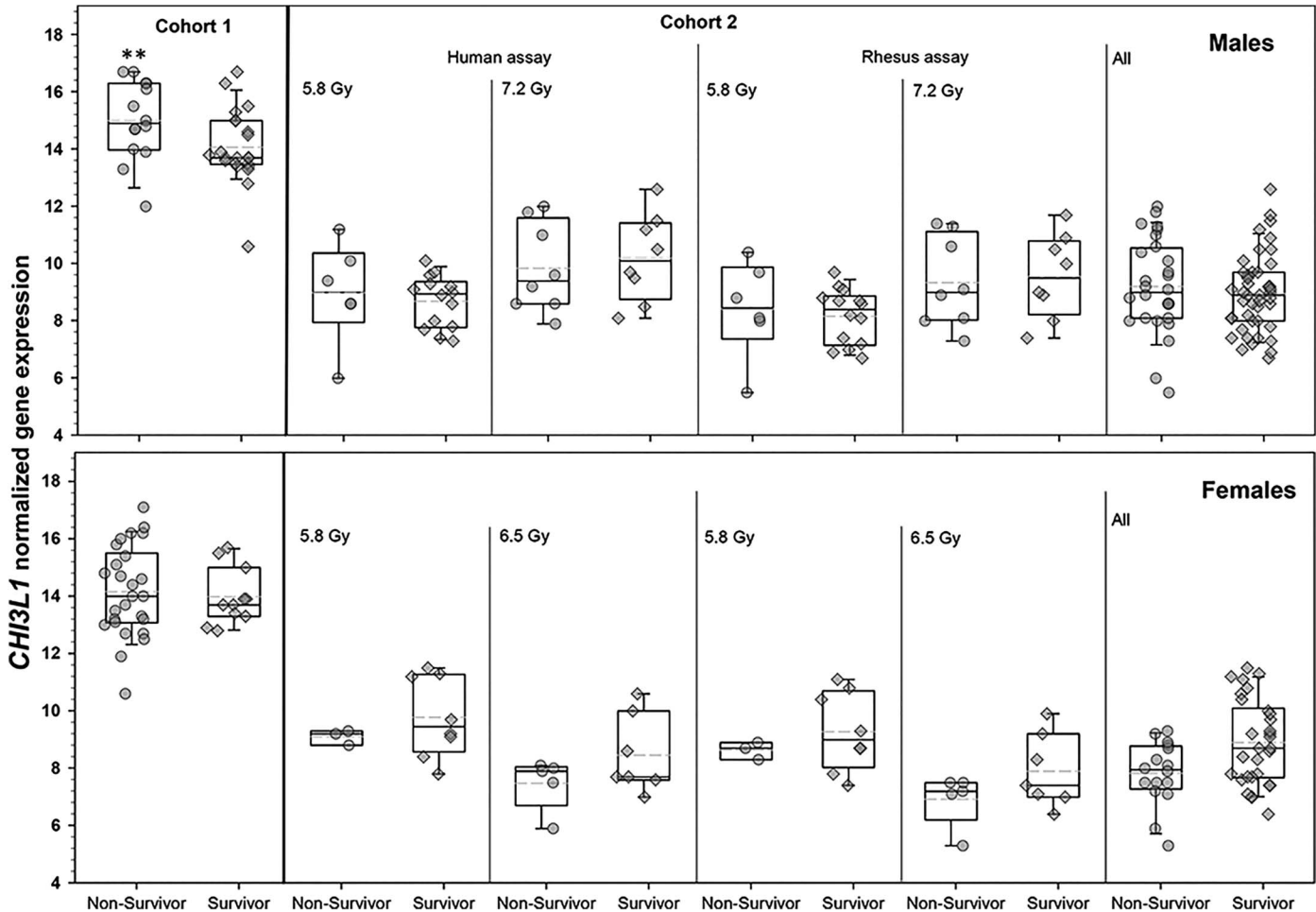
FIG. 1. Normalized *CHI3L1* gene expression (GE) Ct values are shown for survivors and non-survivors of two irradiated rhesus macaque cohorts, separated for males (upper graph) and females (lower graph). Two different TaqMan assays (human and rhesus) for gene identification were employed. Comparisons on gene expression were performed for different exposures indicated as absorbed doses in Gy. Finally, all measurements for cohort 2 were merged and depicted in the right part of the graphs. Asterisks represent the statistically significant comparison of mean or median *CHI3L1* GE values between survivors and non-survivors with $*0.1 > P \geq 0.05$, $**0.05 > P \geq 0.01$, and $***P < 0.01$. Details regarding P values are shown in Table 2.

graphical presentations, SAS (release 9.4, Cary NC) and Excel (Microsoft, Redmond, CA), as well as SPW (SigmaPlot, Version 14.5, Jandel Scientific, Erkrath, Germany) and PowerPoint (Microsoft) were used.

RESULTS

Significant and borderline significant differences in RNA copy numbers (normalized Ct values) between survivors and non-survivors could only be validated for *CHI3L1* and *CHD5* when merging all rhesus macaques regardless of the treatment and the radiation dose of cohort 2 [Table 2 (under cohort 2); Supplementary Table S2 (https://doi.org/10.1667/RADE-23-00099.1.S2) and Supplementary Table S3 (https://doi.org/10.1667/RADE-23-00099.1.S3); Figs. 1 and 2; Supplementary Fig. S1; https://doi.org/10.1667/RADE-23-00099.1.S4] while ignoring sex differences. Examinations considering treatment and radiation exposure revealed significant/borderline significant differences in certain strata, but an expected pattern, e.g., a dose, treatment, or sex dependency, was

not shown (Table 2, lower part; Figs. 1 and 2). In males, deregulation of *CHD5* GE in the same direction could be demonstrated in both cohorts, both doses, as well as both species-specific gene detection assays, but these differences did not reach significance and were less consistent in females (Fig. 2). Throughout, non-survivors revealed a tendency of larger variance in *CHD5* GE compared to the survivors, caused by a subpopulation of rhesus macaques comprising *CHD5* GE values ≤ 11 (Fig. 2). Fold change in *CHD5* GE appeared down-regulated in both sexes and reached significance when merged or examined in females only (Table 3). *CHI3L1* was down-regulated in females (contrary to cohort 1; Fig. 1) and up-regulated in males, leading to insignificant fold change when merged. Univariate (*CHI3L1* and *CHD5* GE examined separately) logistic regression analysis corresponded to fold change differences, and bivariate logistic regression analysis (*CHI3L1* and *CHD5* GE combined) revealed significant/borderline significant contributions of *CHD5* GE,
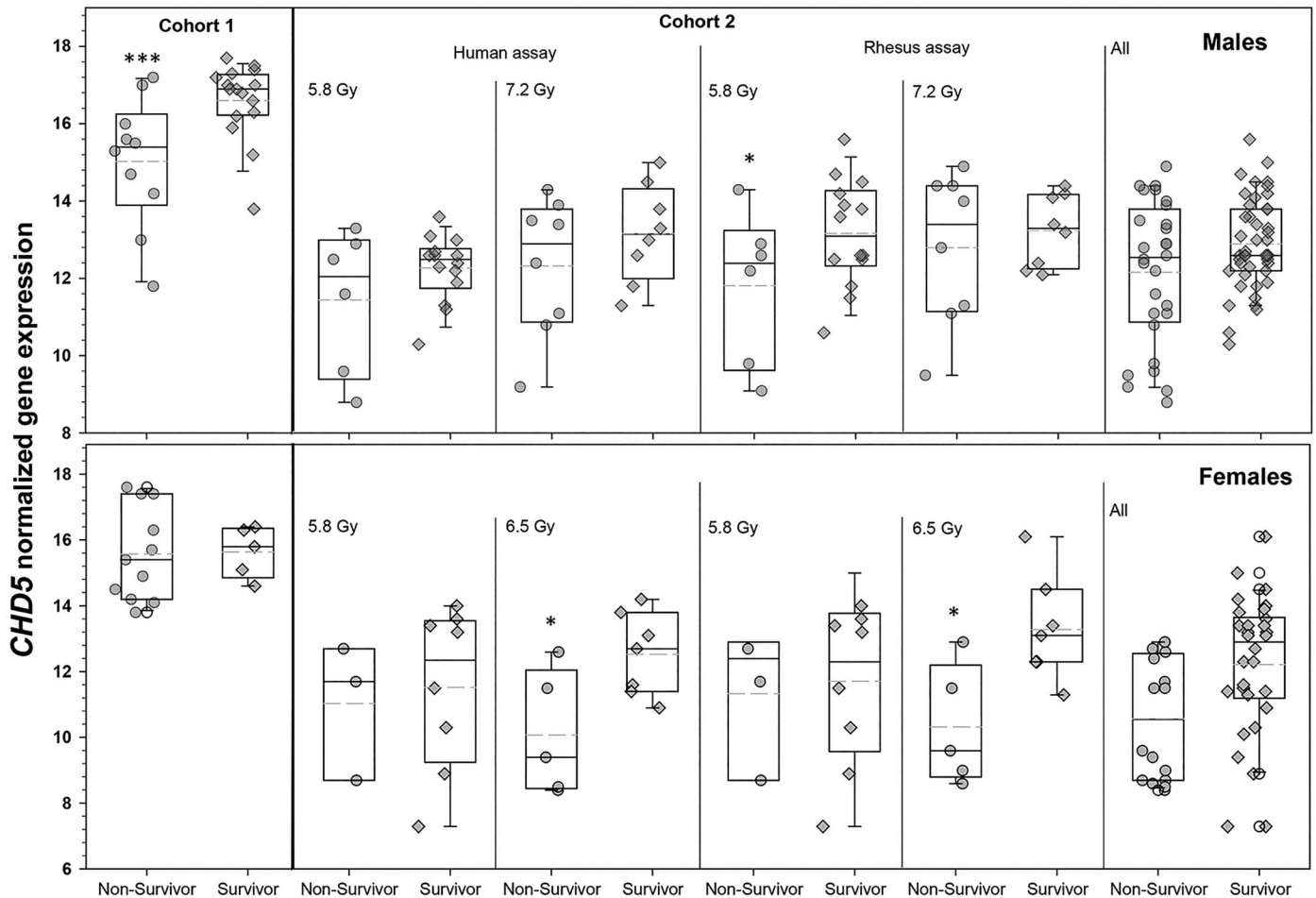
FIG. 2. Normalized *CHD5* gene expression (GE) Ct values are shown for survivors and non-survivors of two irradiated rhesus macaque cohorts, separated for males (upper graph) and females (lower graph). Two different TaqMan assays (human and rhesus) for gene identification were employed. Comparisons on gene expression were performed for different exposures indicated as absorbed doses in Gy. Finally, all measurements for cohort 2 were merged and depicted in the right part of the graphs. Asterisks represent the statistically significant comparison of mean or median *CHD5* GE values between survivors and non-survivors with *$0.1 > P \geq 0.05$, **$0.05 > P \geq 0.01$, and ***$P < 0.01$.

which strengthens with increased sample size in models merging both sexes (Table 3, lower part). Lower P values could be calculated using the rhesus macaque gene detection assays compared to the human assay, and in 48 comparisons, fold changes were comparable among both assays (data not shown). Examination of *CHD5* GE separately for sex, cohort, and both combined strengthened the association with increasing sample size regarding fold change and odds ratio [n = 104, OR 1.38, 95% CI 1.07–1.79, P = 0.01 (Table 4, lower part)]. However, this association was driven by males [OR 1.62, 95% CI 1.10–2.38, P = 0.01 (Table 4 upper part)] and less by females because fold change in the control range were observed in cohort 1 and down-regulated in cohort 2 (Table 4, middle part). When removing *CHD5* Ct values ≤ 11 from these models, all associations became insignificant (Table 4). The ROC curve also shows this for males (Fig. 3). Furthermore, *CHD5* Ct values ≤ 11 were mainly associated with increased frequencies (61–100%) of non-survivors, a trend which depending on the sample numbers comprising

CHD5 Ct values ≤ 11 reached significances (P = 0.03) in males and accordingly in females (Table 5).

A second male subcohort comprising high *CHD5* Ct values ≥ 14.4 in both cohorts (n = 5) appeared associated with survival (Table 5, right side), and removing these high *CHD5* Ct values converted the model borderline significant (P = 0.051; Table 4). Based on the male probability function of the ROC curves, 8 (12.3%) and 5 (7.7%) from 65 pre-exposure RNA measurements in males, death and survival could be predicted with a negative and positive predictive value ranging between 85–100%. An associated odds ratio reflecting a 62% elevated risk for dying or surviving per unit change (Ct value) in gene expression considers the before mentioned *CHD5* thresholds in RNA copy numbers (Fig. 3).

DISCUSSION

Identifying radiosensitive individuals prior to exposure (e.g., a mission to the moon, ARTEMIS) can be beneficial

TABLE 3
The Genes *CHI3L1* and *CHD5* Showed Significant Association with Survival in Both Cohorts

mRNA species	Assay	n (Survivor)	n (Non-Survivor)	Mean Ct-value (Survivor)	Mean Ct-value (Non-Survivor)	Fold change	p-value	Model	Odds ratio	95% CI	p-value	ROC
											Logistic regression	
Males (all samples)												
CHI3L1	Hs	26	14	9.3	9.5	1.2	0.6	univariate	0.9	0.6 1.4	0.6	0.54
CHI3L1	Rm	26	14	8.7	8.9	1.2	0.6	univariate	0.9	0.5 1.4	0.6	0.54
CHD5	Hs	25	14	12.5	12.0	0.7	0.2	univariate	1.4	0.8 2.2	0.2	0.57
CHD5	Rm	26	14	13.2	12.4	0.6	0.2	univariate	1.4	0.9 2.2	0.1	0.57
CHI3L1 & CHD5 combined	Hs	25	14					bivariate	0.7	0.4 1.2	0.2	
									1.7	0.9 3.0	*0.09*	
											0.2	0.64
CHI3L1 & CHD5 combined	Rm	26	14					bivariate	0.7	0.4 1.2	0.2	
									1.7	0.98 2.9	*0.06*	
											0.2	0.64
Females (all samples)												
CHI3L1	Hs	15	8	9.2	8.1	0.48	*0.09*	univariate	1.9	0.9 4.2	0.1	0.67
CHI3L1	Rm	15	8	8.6	7.6	0.48	*0.09*	univariate	1.9	0.9 4.1	0.1	0.67
CHD5	Hs	15	8	12.0	10.4	0.34	*0.09*	univariate	1.5	0.9 2.4	*0.096*	0.73
CHD5	Rm	15	8	12.4	10.7	0.30	*0.08*	univariate	1.5	0.9 2.3	*0.09*	0.74
CHI3L1 & CHD5 combined	Hs	15	8					bivariate	1.8	0.8 4.1	0.1	
									1.5	0.9 2.5	0.1	
											0.1	0.78
CHI3L1 & CHD5 combined	Rm	15	8					bivariate	1.9	0.9 4.3	0.1	
									1.5	0.9 2.4	*0.09*	
											0.097	0.83
Both sexes (all samples)												
CHI3L1	Hs	40	22	9.2	9.0	0.8	0.50	univariate	1.1	0.8 1.7	0.5	0.55
CHI3L1	Rm	41	22	8.7	8.4	0.8	0.52	univariate	1.1	0.8 1.6	0.5	0.54
CHD5	Hs	40	22	12.3	11.4	0.52	*0.04*	univariate	1.4	**1.0 1.9**	*0.046*	0.63
CHD5	Rm	41	22	12.9	11.8	0.46	*0.02*	univariate	1.4	**1.0 1.9**	*0.03*	0.65
CHI3L1 & CHD5 combined	Hs	40	22					bivariate	1.0	**0.7 1.5**	1.0	
									1.4	**1.0 2.0**	*0.06*	
											0.1	0.63
CHI3L1 & CHD5 combined	Rm	41	22					bivariate	1.0	**0.7 1.5**	1.0	
									1.4	**1.0 1.9**	*0.04*	
											0.1	0.65

A further characterization of cohort 2 data is shown here. Descriptive statistics include the number of measurements in survivors and non-survivors, mean gene expression values, calculated fold-changes (with non-survivors used as the reference), and P values are combined with univariate or bivariate logistic regression models (right side of the table). Measurements and calculations are provided for the human (Hs) and the rhesus macaque (Rm) TaqMan gene detection assays separately for males, females, and both combined.

to more accurately assess the individual health risk of individuals exposed to ionizing radiation medically, occupationally or accidentally. Previous work of our group on 122 rhesus macaques identified eight genes significantly associated with survival after radiation exposure, where 66% of the animals survived (*18*). Accessing a second irradiated rhesus macaques cohort comprising 40 male and 23 female animals provided an opportunity for independent validation of these radiosensitivity-predicting genes. Two out of eight genes, namely *CHI3L1* and *CHD5,* appeared significantly associated with survival, as well. Although radiation-induced gene expression changes for *CHI3L1* showed opposing directions in both cohorts, leaving only *CHD5* eligible for further analysis. Expected associations with dose or treatment were not found. Instead, another pattern evolved: The association of *CHD5* GE with non-survival strengthened with increasing sample size and examining both cohorts and sexes combined. The association was driven by a subpopulation of males comprising *CHD5* Ct values ≤ 11. With increasing sample size, the total number (n = 17) of animals comprising *CHD5* Ct values ≤ 11 increased as well (Table 2). These values were mostly associated with increased frequencies (61–100%) of male non-survivors (Table 5). When removed this subgroup from logistic regression models, all significant associations of *CHD5* with survival became insignificant (Tables 2 and 4; Fig. 3). Another subpopulation (n = 5) of male rhesus macaques comprising *CHD5* Ct values ≥ 14.4 was only found in survivors and both cohorts (Table 5). Removing these values reverted the association to borderline significant. Based on these findings, predictions regarding radiosensitivity (dying)/radioresistance (surviving) can be provided for about 20% of males in both cohorts with an 85–100% likelihood (Fig. 3).

TABLE 4
A Further Characterization of *CHD5* Gene Expression (GE) Data Only is Shown Here. For this Comparison, *CHD5* GE Values Measured with Different qrt-PCR Techniques in Both Cohorts had to be Aligned (for Details, See Material and Method Part)

Sex	Cohort	n (survivor)	n (nonsurvivor)	CHD5 mean Ct-value (survivor)	CHD5 mean Ct-value (nonsurvivor)	Fold change	p-value	Logistic regression			
								Odds ratio	95% CI	p-value	ROC
Males	1	16	10	13.6	12.0	0.3	*0.006*	2.6	1.1 6.1	*0.03*	0.79
	2	25	14	12.5	12.0	0.7	0.3	1.4	0.8 2.2	0.2	0.57
	1&2	41	24	13.0	12.0	0.5	*0.009*	1.6	1.1 2.4	*0.01*	0.66
	1&2, excluding Ct ≤ 11	39	18	13.1	12.8	0.8	0.4	1.3	0.7 2.2	0.36	0.58
	1&2, excluding Ct ≥ 14.4	36	24	12.7	12.0	0.6	0.07	1.5	1.0 2.2	*0.05*	0.62
	1&2, excluding 11 ≥ Ct ≥ 14.4	34	18	12.9	12.8	1.0	0.9	1.0	0.6 1.9	0.88	0.52
Females	1	5	11	15.6	15.6	1.0	0.9	1.1	0.4 2.5	0.9	0.58
	2	15	8	12.0	10.4	0.3	*0.09*	1.5	0.9 2.4	*0.096*	0.73
	1&2	20	19	12.2	11.7	0.7	0.4	1.2	0.8 1.6	0.4	0.60
	1&2, excluding Ct ≤ 11	16	14	12.9	12.6	0.8	0.50	1.3	0.6 2.6	0.5	0.60
	1&2, excluding Ct ≤ 14.4	20	16	12.8	11.5	0.4	**0.03**	1.4	0.9 2.2	*0.1*	0.71
	1&2, excluding 11 ≥ Ct ≥ 14.4	16	11	12.9	12.1	0.6	**0.03**	3.0	1.1 8.2	*0.037*	0.76
Both sex	1	21	21	16.4	15.3	0.48	*0.01*	1.9	1.1 3.3	*0.02*	0.70
	2	40	22	12.3	11.4	0.5	*0.04*	1.4	1.0 1.9	*0.046*	0.63
	1&2	61	43	12.7	11.9	0.6	*0.02*	1.4	1.1 1.8	*0.01*	0.64
	1&2, excluding Ct ≤ 11	55	32	13.0	12.7	0.8	0.2	1.3	0.9 2.0	0.20	0.58

Descriptive statistics include the number of measurements in survivors and non-survivors, mean gene expression values, calculated fold-changes (with non-survivors used as the reference), and P values combined with univariate logistic regression models (right side of the table). Measurements and calculations are provided for the human TaqMan gene detection assay only. These measurements were performed for each cohort, combining both cohorts and excluding subgroups of measurements as stated.
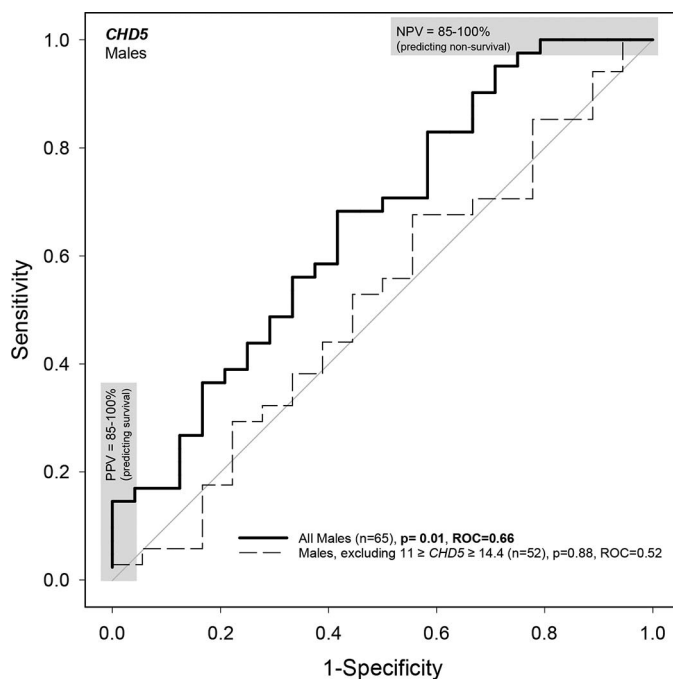

FIG. 3. *CHD5* gene expression (GE) measurements of both cohorts were merged, and ROC curves for males were generated. Two ROC curves reflect data generated on all males (bold black line) (ROC = 0.66), males excluding *CHD5* > 11 and *CHD5* ≥ 14.4 (medium dashed line) (ROC = 0.52), gray boxes mark the area of positive (PPV, lower right) and negative predictive values (NPV, upper right), thus predicting survival and non-survival with 85–100%, respectively.

Predicting opposing biological effects (dying or surviving) depending on increased or decreased *CHD5* copy numbers in male pre-exposure peripheral blood samples might reflect a causal relationship. The results confirm that the pre-exposure transcription status of the cells at the time of radiation exposure would impact survival or non-survival. Nevertheless, no correlation between radiosensitivity and dose or treatment was found by investigating the rhesus macaque cohort. This can be explained by the simple fact that rhesus macaques were not selected into treatment or radiation exposure groups based on their pre-exposure CHD5 RNA copy numbers. Consequently, the missing association appears more by chance, strengthen when examining all animals including the identified *CHD5* subcohort (see Table 4 and Fig. 3) and is therefore in line with our hypothesis.

The validated gene *CHD5* belongs to the class II, chromodomain helicase DNA (CHD)-binding proteins (*35*). They are important influencers of radiation-induced signaling transduction pathways and the oxidative stress-induced DNA-double strand break repair (*36, 37*). Several studies indicate an impact of *CHD5* on the G_1/S-phase gatekeeper p53 by transcriptional regulations via the cyclin-dependent kinase inhibitor 2A locus (*CDK2A*) (*38–40*) (Fig. 4). Against this background, *CHD5* plays a role in a wide range of tumor entities in various ways (*40–45*). High expression of *CHD5* leads to cell cycle arrest and apoptosis in chronic myeloid leukemia patients (*41*) and inhibits renal cancer cells from

TABLE 5
A Frequency Distribution Comparison among *CHD5* Subgroups (*CHD5* ≤ 11, Tables Left Side and *CHD5* ≥ 14.4, Tables Right Side) is Shown for the Number of Survivors and Non-Survivors using All Samples from Both Cohorts and Separately for Each Cohort and Sex

Comparisons	CHD5 normalized Ct-values	Non-survivor #	Percent	Survivor #	Percent	p-value	CHD5 normalized Ct-values	Non-survivor #	Percent	Survivor #	Percent	p-value
All samples from both cohorts (n = 104)												
	CHD5 ≤ 11	11	64.7	6	35.3		CHD5 ≤ 14.4	40	41.7	56	58.3	
	CHD5 > 11	32	36.8	55	63.2	**0.03**	CHD5 > 14.4	3	37.5	5	62.5	0.72
Cohort 1 samples, both sexes (n = 42)												
	CHD5 ≤ 11	3	75	1	25		CHD5 ≤ 14.4	18	50	18	50	
	CHD5 > 11	18	47.4	20	52.6	0.29	CHD5 > 14.4	3	50	3	50	1.0
Cohort 2 samples, both sexes (n = 62)												
	CHD5 ≤ 11	8	61.5	5	38.5		CHD5 ≤ 14.4	22	36.7	38	63.3	
	CHD5 > 11	14	28.6	35	71.4	**0.03**	CHD5 > 14.4	0	0	2	100	1.0
Cohort 1 samples, males only (n = 26)												
	CHD5 ≤ 11	2	66.7	1	33.3		CHD5 ≤ 14.4	10	43.5	13	56.5	
	CHD5 > 11	8	34.8	15	61.5	0.29	CHD5 > 14.4	0	0	3	100	0.26
Cohort 2 samples, males only (n = 39)												
	CHD5 ≤ 11	4	80	1	20		CHD5 ≤ 14.4	14	37.8	23	62.2	
	CHD5 > 11	10	29.4	24	70.6	**0.03**	CHD5 > 14.4	0	0	2	100	0.28
Cohort 1 samples, females only (n = 16)												
	CHD5 ≤ 11	1	100	0	0		CHD5 ≤ 14.4	8	61.5	5	38.5	
	CHD5 > 11	10	68.8	5	31.2	0.49	CHD5 > 14.4	3	100	0	0	0.29
Cohort 2 samples, females only (n = 23)												
	CHD5 ≤ 11	4	50	4	50		CHD5 ≤ 14.4	8	34.8	15	65.2	
	CHD5 > 11	4	26.7	11	73.3	0.26	CHD5 > 14.4	0	0	0	0	nd

Significant P values are bold. Enriched frequencies of non-survivors associated with *CHD5* ≤ 11 values and survivors associated with *CHD5* ≥ 14.4 values are highlighted in gray boxes.

further growth and invasion (*40*). In this light, already high pre-exposure *CHD5* copy numbers could predispose the whole organism to death via additional radiation-induced up-regulation of *CHD5*. This finally leads to the p53 activation and consecutive cell-cycle arrest and apoptosis. To prove this hypothesis, further validation experiments are needed.

A gene detection assay based on the human genome was employed in rhesus macaque in the previous cohort 1 study to translate rhesus macaque results into the human species better. For the second validation cohort, complimentary gene detection assays using the rhesus macaque transcriptome were generated. Both species-specific assays showed similar results with slightly improved P values when using the rhesus macaque assays. This confirms the performed measurements and reflects the known homology of both genomes.

Our study bears limitations leaving space for alternative interpretations of our data. Although two rhesus macaque cohorts with a total of 185 animals were examined (including 104 rhesus macaques with *CHD5* measurements), only 17 animals showed *CHD5* Ct values ≤ 11, and 8 animals showed *CHD5* Ct values ≥ 14.4. These groups were identified as the "driver" of statistically significant results in all data combined, as well as male models (n = 8 and n = 5 for both *CHD5* threshold values mentioned above). However, in females and cohort 2, half of rhesus macaques with *CHD5* Ct values ≤ 11 were associated with non-survivors and the other half with survivors (Table 5). In contrast, male *CHD5* Ct values ≤ 11 showed higher frequencies in non-survivors than survivors. For *CHD5* Ct values ≥ 14.4, all male rhesus macaques were survivors in both cohorts, unlike the females in cohort 1, where all were non-survivors (Table 5). Hence, a gender effect or a significant association by chance must be considered. Interestingly, after deleting 11≥ *CHD5* ≥ 14.4 in females, a significant association (P = 0.04) of remaining *CHD5* measurements could be found, and the ROC area increased to 0.76 (data not shown). This might indicate a gender-dependent effect with other *CHD5* thresholds for females. Further studies in this regard are required. Our Gnostic analysis approach to predict pre-exposure radiosensitivity is limited because we are focusing on a set of genes. Therefore, we do not depict a complementary bioinformatics approach, where networks of genes are considered. This restriction could explain the identified result differences between both cohorts. In theory, even one gene which was not considered in our previous analysis in cohort one, but altered in cohort two, could modify the network and affect the expected radiosensitivity outcome prediction of our examined candidate genes.
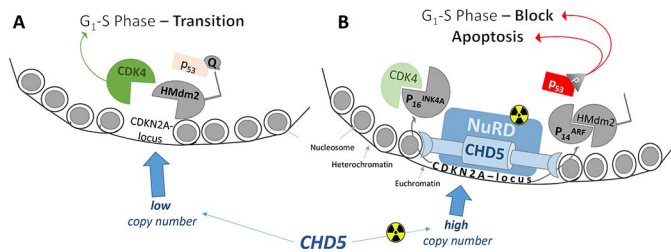
FIG. 4. Panel A: Shows the normal cell cycle progression with low *CHD5* copy-numbers and homeostasis of factors promoting cell cycle progression as well as arrest, resulting in a controlled G_1-S phase transition. *CDKN2A*-locus is condensed and, this way, not readable for transcription factors. Homolog mouse double minute 2 protein (HMdm2) with its E3-ubiquitin-protein ligase activity can ubiquitinate p53 for degradation, which cannot slow cell cycle progression down (*38, 46*). Panel B: Shows the process in the presence of high copy numbers of *CHD5* as a component of Nucleosome remodeling and deacetylase complex (NuRD). The NuRD with *CHD5* specifically interacts with *CDKN2A*-locus in terms of DNA damage due to several Noxa (*38, 39*) as well as ionizing radiation. In this way, transcription factors can access *CDKN2A*-locus, and P_{16}^{INK4A}, as well as P_{14}^{ARF} are produced. This inhibits cyclin-dependent kinase 4 (*CDK4*) and sequesters HMdm2, respectively. HMdm2 cannot ligate Ubiquitin (Q) to p53, which is activated by phosphorylation (P). In combination, this leads to a blocked G_1-S phase transition, resulting in cell cycle arrest and apoptosis (*46*).

In summary, using two species specific gene detection assays, similar gene expression results were generated, thus, confirming the performed measurements. Only one (*CHD5*) from eight genes could be independently validated in two rhesus macaque cohorts. Significant associations of *CHD5* GE with survival were driven by male subgroups comprising either higher *CHD5* copy numbers in pre-exposure peripheral blood samples with a predisposition to die or lowered *CHD5* copy numbers with a predisposition to survive after irradiation. Predictions regarding radiosensitivity (dying) and radioresistance (surviving) could be provided for about 20% of males in both cohorts. These findings might reflect a causal relationship and require further research.

SUPPLEMENTARY MATERIALS

Supplementary Table S1. The table provides an overview of raw and normalized Ct values of eight genes examined with a human (Hs) and a rhesus (Rm) specific TaqMan gene expression detection assay for each of the 63 examined rhesus macaque of cohort 2. Further characteristics such as sex (males, m; females f), H-ARS severity category, treatment regimen (gamma-tocotrienol, GT3), and dose are provided.

Supplementary Table S2. The table provides an overview of sample numbers of survivors and non-survivors, mean normalized Ct values, and corresponding fold-change calculations of eight genes examined with a human-specific TaqMan gene expression detection assay in two cohorts and separately for males (m) and females (f). Significant P values are presented in bold.

Supplementary Table S3. The table provides an overview of the human and corresponding rhesus macaques TaqMan Assays used within this study.

Supplementary Fig. S1. Normalized gene expression (GE) Ct values from six genes, namely *DYSF, EPX, IGF2BP1, LCN2, MBOAT4*, and *SLC22A4* (referred to as Fig. 1A–F), are shown for survivors and non-survivors of two irradiated rhesus macaque cohorts and separately for males (upper graph) and females (lower graph). Two different TaqMan assays (human and rhesus assays) for gene identification were employed. Comparisons on gene expression were performed for different exposures indicated as absorbed doses in Gy. Finally, all measurements for cohort 2 were merged and depicted in the right part of the graphs.

REFERENCES

1. Hall EJ. Radiation, the two-edged sword: cancer risks at high and low doses. Cancer J. 2000; 6(6):343–50.

2. Hall EJ, Giaccia AJ. Radiobiology for the radiologist: Seventh edition. 2012. 1–576 p.

3. Port M, Majewski M, Abend M. Radiation Dose Is of Limited Clinical Usefulness in Persons with Acute Radiation Syndrome. Radiat Prot Dosimetry. 2019; 186(1):126–9. doi:10.1093/rpd/ncz058

4. Zhang S, Wimmer-Schweingruber RF, Yu J, Wang C, Fu Q, Zou Y, et al. First measurements of the radiation dose on the lunar surface. Sci Adv. 2020; 6(39). doi:10.1126/sciadv.aaz1334

5. Herskind C, Talbot CJ, Kerns SL, Veldwijk MR, Rosenstein BS, West CM. Radiogenomics: A systems biology approach to understanding genetic risk factors for radiotherapy toxicity? Cancer Lett. 2016; 382(1):95–109. doi:10.1016/j.canlet.2016.02.035

6. Wisdom AJ, Kirsch DG. Functional assay to guide precision radiotherapy by assessing individual patient radiosensitivity. EBioMedicine. 2019; 41:26–7. doi:10.1016/j.ebiom.2019.03.002

7. Moding EJ, Kastan MB, Kirsch DG. Strategies for optimizing the response of cancer and normal tissues to radiation. Nat Rev Drug Discov. 2013; 12(7):526–42. doi:10.1038/nrd4003

8. Cullings HM, Fujita S, Funamoto S, Grant EJ, Kerr GD, Preston DL. Dose estimation for atomic bomb survivor studies: its evolution and present status. Radiat Res. 2006; 166(1 Pt 2):219–54. doi: 10.1667/RR3546.1

9. Strahlenschutzkomission. Geschlechtsspezifische Unterschiede der Strahlenempfindlichkeit – epidemiologische, klinische und biologische Studien. In: BMU - Bundesministerium für Umwelt N, nukleare Sicherheit und Verbraucherschutz, editor. Bundesanzeiger Nr. 93 (Beilage) 2010.

10. Narendran N, Luzhna L, Kovalchuk O. Sex Difference of Radiation Response in Occupational and Accidental Exposure. Front Genet. 2019; 10:260. doi:10.3389/fgene.2019.00260

11. Kheirandish P, Chinegwundoh F. Ethnic differences in prostate cancer. Br J Cancer. 2011; 105(4):481–5. doi:10.1038/bjc.2011.273

12. Rawla P. Epidemiology of Prostate Cancer. World J Oncol. 2019; 10(2):63–89. doi:10.14740/wjon1191

13. Patterson AM, Vemula S, Plett PA, Sampson CH, Chua HL, Fisher A, et al. Age and Sex Divergence in Hematopoietic Radiosensitivity in Aged Mouse Models of the Hematopoietic Acute Radiation Syndrome. Radiat Res. 2022; 198(3):221–42. doi:10.1667/RADE-22-00071.1

14. Beach T, Authier S, Javitz HS, Wong K, Bakke J, Gahagen J, et al. Total body irradiation models in NHPs - consideration of animal sex and provision of supportive care to advance model development. Int J Radiat Biol. 2021; 97(2):126–30. doi:10.1080/09553002.2021.1844335

15. Singh VK, Carpenter AD, Janocha BL, Petrus SA, Fatanmi OO, Wise SY, et al. Radiosensitivity of rhesus nonhuman primates: Consideration of sex, supportive care, body weight and age at time of exposure. Expert Opin Drug Discov. 2023; 18(7):797–814. doi:10.1080/17460441.2023.2205123

16. Port M, Majewski M, Herodin F, Valente M, Drouet M, Forcheron F, et al. Validating Baboon Ex Vivo and In Vivo Radiation-Related Gene Expression with Corresponding Human Data. Radiat Res. 2018; 189(4):389–98. doi:10.1667/RR14958.1

17. Fendler W, Malachowska B, Meghani K, Konstantinopoulos PA, Guha C, Singh VK, et al. Evolutionarily conserved serum microRNAs predict radiation-induced fatality in nonhuman primates. Sci Transl Med. 2017; 9(379):eaal2408. doi:10.1126/scitranslmed.aal2408

18. Ostheim P, Majewski M, Gluzman-Poltorak Z, Vainstein V, Basile LA, Lamkowski A, et al. Predicting the Radiation Sensitivity of Male and Female Rhesus Macaques Using Gene Expression. Radiat Res. 2021; 195(1):25–37. doi:10.1667/RADE-20-00161.1

19. Garg TK, Garg S, Miousse IR, Wise SY, Carpenter AD, Fatanmi OO, et al. Gamma-Tocotrienol Modulates Total-Body Irradiation-Induced Hematopoietic Injury in a Nonhuman Primate Model. Int J Mol Sci. 2022; 23(24). doi:10.3390/ijms232416170

20. Ledet GA, Biswas S, Kumar VP, Graves RA, Mitchner DM, Parker TM, et al. Development of Orally Administered gamma-Tocotrienol (GT3) Nanoemulsion for Radioprotection. Int J Mol Sci. 2016; 18(1). doi:10.3390/ijms18010028

21. Singh VK, Hauer-Jensen M. gamma-Tocotrienol as a Promising Countermeasure for Acute Radiation Syndrome: Current Status. Int J Mol Sci. 2016; 17(5). doi:10.3390/ijms17050663

22. Singh VK, Kulkarni S, Fatanmi OO, Wise SY, Newman VL, Romaine PL, et al. Radioprotective Efficacy of Gamma-Tocotrienol in Nonhuman Primates. Radiat Res. 2016; 185(3):285–98. doi:10.1667/RR14127.1

23. Singh VK, Seed TM. Development of gamma-tocotrienol as a radiation medical countermeasure for the acute radiation syndrome: current status and future perspectives. Expert Opin Investig Drugs. 2023:1–11. doi:10.1080/13543784.2023.2169127

24. Phipps AJ, Bergmann JN, Albrecht MT, Singh VK, Homer MJ. Model for Evaluating Antimicrobial Therapy To Prevent Life-Threatening Bacterial Infections following Exposure to a Medically Significant Radiation Dose. Antimicrob Agents Chemother. 2022; 66(10):e0054622. doi:10.1128/aac.00546-22

25. Garg S, Garg TK, Wise SY, Fatanmi OO, Miousse IR, Savenka AV, et al. Effects of Gamma-Tocotrienol on Intestinal Injury in a GI-Specific Acute Radiation Syndrome Model in Nonhuman Primate. Int J Mol Sci. 2022; 23(9). doi:10.3390/ijms23094643

26. Carpenter AD, Li Y, Janocha BL, Wise SY, Fatanmi OO, Maniar M, et al. Analysis of the proteomic profile in serum of irradiated nonhuman primates treated with Ex-Rad, a radiation medical countermeasure. J Proteome Res. 2023; 22:1116–26. doi:10.1021/acs.jproteome.2c00458

27. National Research Council of the National Academy of Sciences. Guide for the care and use of laboratory animals. 8th ed. Washington, DC: National Academies Press; 2011.

28. Garg S, Garg TK, Miousse IR, Wise SY, Fatanmi OO, Savenka V, et al. Effects of gamma-tocotrienol on partial-body irradiation-induced intestinal injury in a nonhuman primate model. Antioxidants. 2022; 11(10):1895. doi:10.3390/antiox11101895

29. Li Y, Singh J, Varghese R, Zhang Y, Fatanmi OO, Cheema AK, et al. Transcriptome of rhesus macaque (Macaca mulatta) exposed to total-body irradiation. Sci Rep. 2021; 11(1):6295. doi:10.1038/s41598-021-85669-6

30. Pannkuk EL, Laiakis EC, Garcia M, Fornace AJ, Jr., Singh VK. Nonhuman primates with acute radiation syndrome: Results from a global serum metabolomics study after 7.2 Gy total-body irradiation. Radiat Res. 2018; 190(5):576–83. doi:10.1667/RR15167.1

31. Pannkuk EL, Laiakis EC, Fornace AJ, Jr., Fatanmi OO, Singh VK. A metabolomic serum signature from nonhuman primates treated with a radiation countermeasure, gamma-tocotrienol, and exposed to ionizing radiation. Health Phys. 2018; 115(1):3–11. doi:10.1097/HP.0000000000000776

32. Vellichirammal NN, Sethi S, Pandey S, Singh J, Wise SY, Carpenter AD, et al. Lung transcriptome of nonhuman primates exposed to total- and partial-body irradiation. Mol Ther Nucleic Acids. 2022; 29:584–98. doi:10.1016/j.omtn.2022.08.006

33. Singh VK, Fatanmi OO, Wise SY, Carpenter AD, Olsen CH. Determination of lethality curve for cobalt-60 gamma-radiation source in rhesus macaques using subject-based supportive care. Radiat Res. 2022; 198(6):599–614. doi:10.1667/RADE-22-00101.1

34. Taylor SC, Nadeau K, Abbasi M, Lachance C, Nguyen M, Fenrich J. The Ultimate qPCR Experiment: Producing Publication Quality, Reproducible Data the First Time. Trends Biotechnol. 2019; 37(7):761–74. doi:10.1016/j.tibtech.2018.12.002

35. Saha A, Wittmeyer J, Cairns BR. Chromatin remodelling: the industrial revolution of DNA around histones. Nat Rev Mol Cell Biol. 2006; 7(6):437–47. doi:10.1038/nrm1945

36. Goodarzi AA, Kurka T, Jeggo PA. KAP-1 phosphorylation regulates CHD3 nucleosome remodeling during the DNA double-strand break response. Nat Struct Mol Biol. 2011; 18(7):831–9. doi:10.1038/nsmb.2077

37. Larsen DH, Poinsignon C, Gudjonsson T, Dinant C, Payne MR, Hari FJ, et al. The chromatin-remodeling factor CHD4 coordinates signaling and repair after DNA damage. J Cell Biol. 2010; 190(5):731–40. doi:10.1083/jcb.200912135

38. Bagchi A, Papazoglu C, Wu Y, Capurso D, Brodt M, Francis D, et al. CHD5 is a tumor suppressor at human 1p36. Cell. 2007; 128(3):459–75. doi:10.1016/j.cell.2006.11.052

39. Stanley FK, Moore S, Goodarzi AA. CHD chromatin remodelling enzymes and the DNA damage response. Mutat Res. 2013; 750(1-2):31–44. doi:10.1016/j.mrfmmm.2013.07.008

40. Huang S, Yan Q, Xiong S, Peng Y, Zhao R, Liu C. Chromodomain Helicase DNA-Binding Protein 5 Inhibits Renal Cell Carcinoma Tumorigenesis by Activation of the p53 and RB Pathways. Biomed Res Int. 2020; 2020:5425612. doi:10.1155/2020/5425612

41. Xiong S, Yan Q, Peng Y, Huang S, Zhao R. Overexpression of chromodomain helicase DNA binding protein 5 (CHD5) inhibits cell proliferation and induces cell cycle arrest and apoptosis in chronic myeloid leukemia. Transl Cancer Res. 2021; 10(2):768–78. doi:10.21037/tcr-20-2276

42. Wong RR, Chan LK, Tsang TP, Lee CW, Cheung TH, Yim SF, et al. CHD5 Downregulation Associated with Poor Prognosis in Epithelial Ovarian Cancer. Gynecol Obstet Invest. 2011; 72(3):203–7. doi:10.1159/000323883

43. Pei S, Chen Z, Tan H, Fan L, Zhang B, Zhao C. SLC16A1-AS1 enhances radiosensitivity and represses cell proliferation and invasion by regulating the miR-301b-3p/CHD5 axis in hepatocellular carcinoma. Environ Sci Pollut Res Int. 2020; 27(34):42778–90. doi:10.1007/s11356-020-09998-1

44. Hall WA, Petrova AV, Colbert LE, Hardy CW, Fisher SB, Saka B, et al. Low CHD5 expression activates the DNA damage response and predicts poor outcome in patients undergoing adjuvant therapy for resected pancreatic cancer. Oncogene. 2014; 33(47):5450–6. doi:10.1038/onc.2013.488

45. Wang L, He S, Tu Y, Ji P, Zong J, Zhang J, et al. Downregulation of chromatin remodeling factor CHD5 is associated with a poor prognosis in human glioma. J Clin Neurosci. 2013; 20(7):958–63. doi:10.1016/j.jocn.2012.07.021

46. Van Maerken T, Vandesompele J, Rihani A, De Paepe A, Speleman F. Escape from p53-mediated tumor surveillance in neuroblastoma: switching off the p14(ARF)-MDM2-p53 axis. Cell Death Differ. 2009; 16(12):1563–72. doi:10.1038/cdd.2009.138